MountainZebra: Real-Time Archival and 4D Visualization of Radar Volumes Over Complex Terrain

Curtis James, Stacy Brodzik, Harry Edmon, Robert Houze, and Sandra Yuter

Department of Atmospheric Sciences, University of Washington

ABSTRACT

MountainZebra is a visualization and data handling system built around NCAR's *Zebra* software, which displays radar volumes interpolated to a Cartesian grid and allows arbitrary vertical and horizontal cross-section analysis. *MountainZebra* adds a high-resolution terrain height field to the basic *Zebra* and thus allows cross-sections to include the terrain profile along with the radar data. This allows velocity and reflectivity fields to be analyzed in precise relation to the topography. *MountainZebra* is being tested in the Seattle National Weather Service Forecast Office (NWSFO) and at the University of Washington. This paper describes the data acquisition and processing procedure and gives examples of structures that have been observed using this technique.

1. INTRODUCTION

We have configured a visualization and data handling system, known as *MountainZebra*, for simultaneous display of radar data and orography. This system is built around *Zebra*, a software package developed by NCAR's Research Data Program (Corbet, et al., 1994). *Zebra* has real-time capability and the ability to ingest and overlay multiple diverse data sets. *MountainZebra* will be particularly useful for operational radar meteorology in mountainous regions. This system is currently being tested with real-time Doppler radar data from the WSR-88D (Weather Surveillance Radar-88D) located approximately 50 km north-northwest of Seattle, Washington, USA. It will also be used to direct aircraft operations in the Mesoscale Alpine Programme (MAP). The purpose of this paper is to show how the incorporation of the terrain-height field into a radar-data visualization system enhances its usefulness. We first present an overview of the automated data acquisition, ingestion, and archival processes associated with *MountainZebra* as configured at the University of Washington for analysis of local WSR-88D radar data. Then, we describe several examples which illustrate *MountainZebra*'s application in the interpretation of orographically-influenced precipitation.

2. OVERVIEW

As shown in Fig. 1, there are three main hardware components to the WSR-88D radar system. Raw analog radar returns (or Level I products) are obtained at the Radar Data Acquisition (RDA) site. The RDA system converts the received signal to reflectivity, radial velocity, and spectral width data in polar coordinates and archives these data to exabyte tape. These polar data are referred to as "Level II" products (Crum and Alberty, 1993). The Level II data are then transmitted to the Radar Product Generator (RPG), where various graphical (Level III) products are produced for display at the National Weather Service and for dissemination to commercial data providers.

When the WSR-88D radars were first installed, investigators could only obtain Level II data by

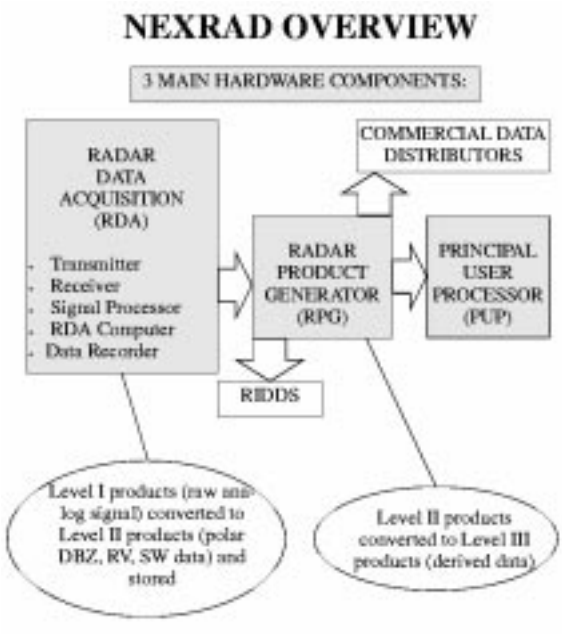

Figure 1. Flow chart depicting the Camano Island WSR-88D data processing from Level I to Level III.

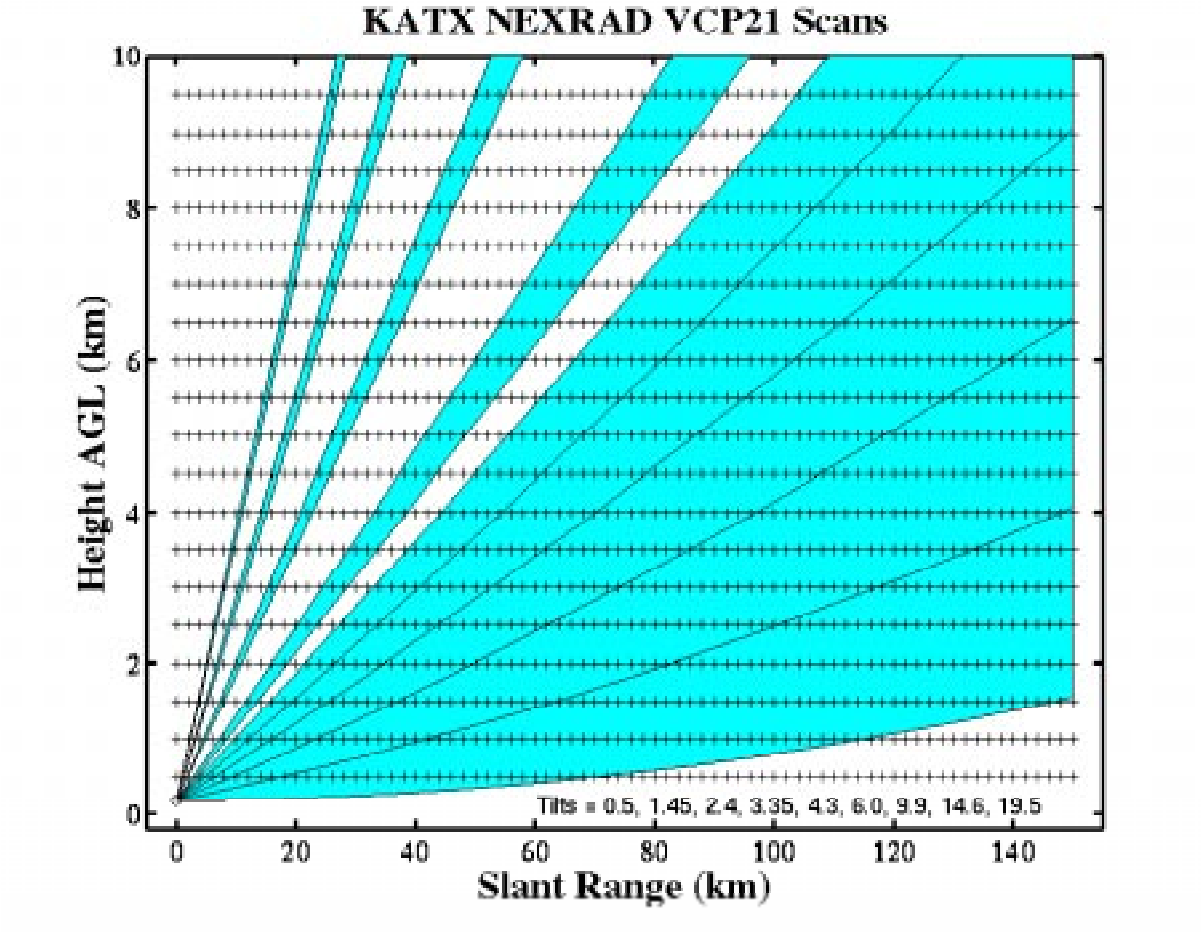

Figure 2.Vertical slice through a typical WSR-88D volume scan taken from Camano Island to 150 km east of the radar. Observed regions are shaded, while data void regions are white. The location of each grid point on the Cartesian grid is indicated by a cross (+). The location of the radar dome is plotted as an open circle.

requesting tapes from the Level II exabyte archive at the National Climatic Data Center. The National Severe Storms Laboratory developed the Radar Interface and Data Distribution System (RIDDS) as a means of accessing Level II radar data in parallel with the Level III product generation within the RPG. A RIDDS workstation installed at the Seattle National Weather Service Forecast Office sends each Level II ray into a circular buffer where packages of several rays of radar data are formed, compressed and queued for transmission to the Department of Atmospheric Sciences at the University of Washington. The data are transmitted over T1 line to a workstation at the department where they are uncompressed and assembled back into Level II volumes. A workstation dedicated to the processing and display of the radar volumes copies the latest Level II files from disk and converts them to Universal Format (Barnes, 1980). At this point, non-precipitation echoes are removed and aliased velocities are corrected by an automatic quality control algorithm.

Finally, the edited reflectivity and radial velocity data are bilinearly interpolated to a Cartesian grid (2 km x 2 km x 0.5 km) using NCAR SPRINT software (Mohr and Vaugn 1979) and converted to NetCDF (Network Common Data Form). Fig. 2 depicts a vertical cross-section of a typical WSR-88D volume coverage pattern (VCP 21) with standard atmosphere refraction applied. The location of each grid point along the cross-section is indicated by '+'. From this figure it is evident that there are inherent problems in interpolating the conical scans to a Cartesian grid. Many grid points are located in data-void regions, leading to concentric rings of missing data in some of the constant-altitude plots. Since the resolution volume size increases with range, the vertical and horizontal structures of the precipitation are not well sampled by the radar at far range. On the other hand, at ranges of less than approximately 20 km, the Cartesian grid does not adequately resolve all of the available scans.

Nevertheless, interpolating the data to a Cartesian grid is desirable. First, it allows any arbitrary horizontal or vertical cross-section to be computed. Second, it

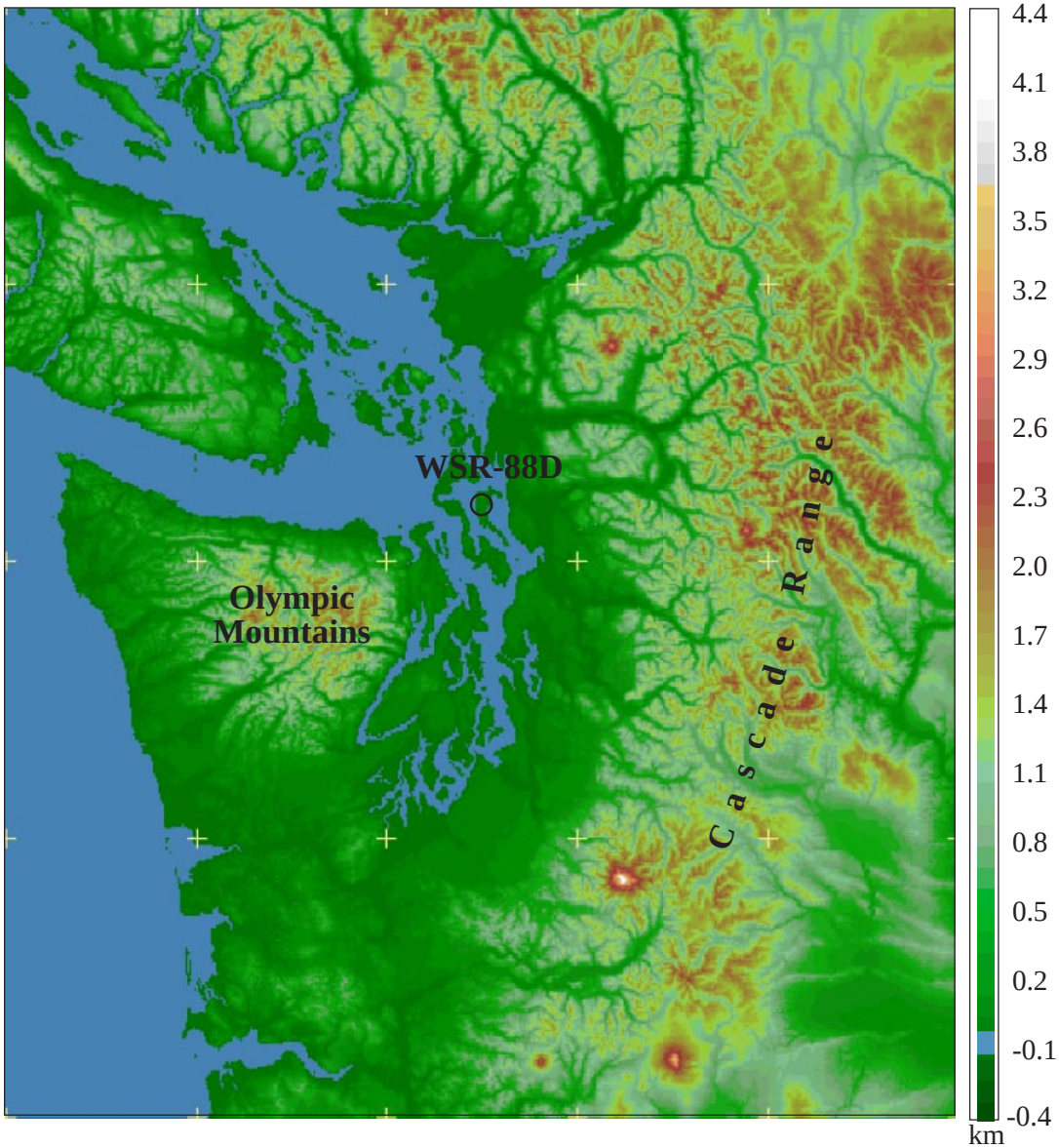

Figure 3. Terrain map indicating the location of the Camano Island WSR-88D in relation to the Olympic Mountains and Cascade Range. Zero elevation is highlighted steel blue.

makes analysis more intuitive. Third, it facilitates statistical and diagnostic computations. Fourth, it is geometrically better suited for analyzing horizontally-aligned structures such as bright bands and stratiform precipitation.

Each radar volume is ingested and displayed in *Zebra* within 5 to 8 min of the completion of the volume scan. Besides the ability to synthesize multiple data sets and create arbitrary cross-sections, *Zebra* allows the user to compile time-lapse movies and easily reference past data sets. Topographical data (<1 km horizontal resolution) can be displayed and viewed simultaneously with the radar, satellite, and other fields in any horizontal or vertical cross section selected by the user. These capabilities provide four-dimensional interpretation of precipitation system structure in relation to terrain shape, dynamic and thermodynamic fields, and satellite measurements.

On a weekly basis, the radar volumes are UNIX compressed and archived on tape in both Level II and Universal Format. The corrected and interpolated data in NetCDF are archived when deemed meteorologically significant.

3. EXAMPLES

The *MountainZebra* visualization system facilitates the interpretation and analysis of precipitation system structure with respect to the terrain. It also allows the observer to identify errors and signals in the reflectivity and radial velocity fields that are caused by the terrain. This can be demonstrated by the

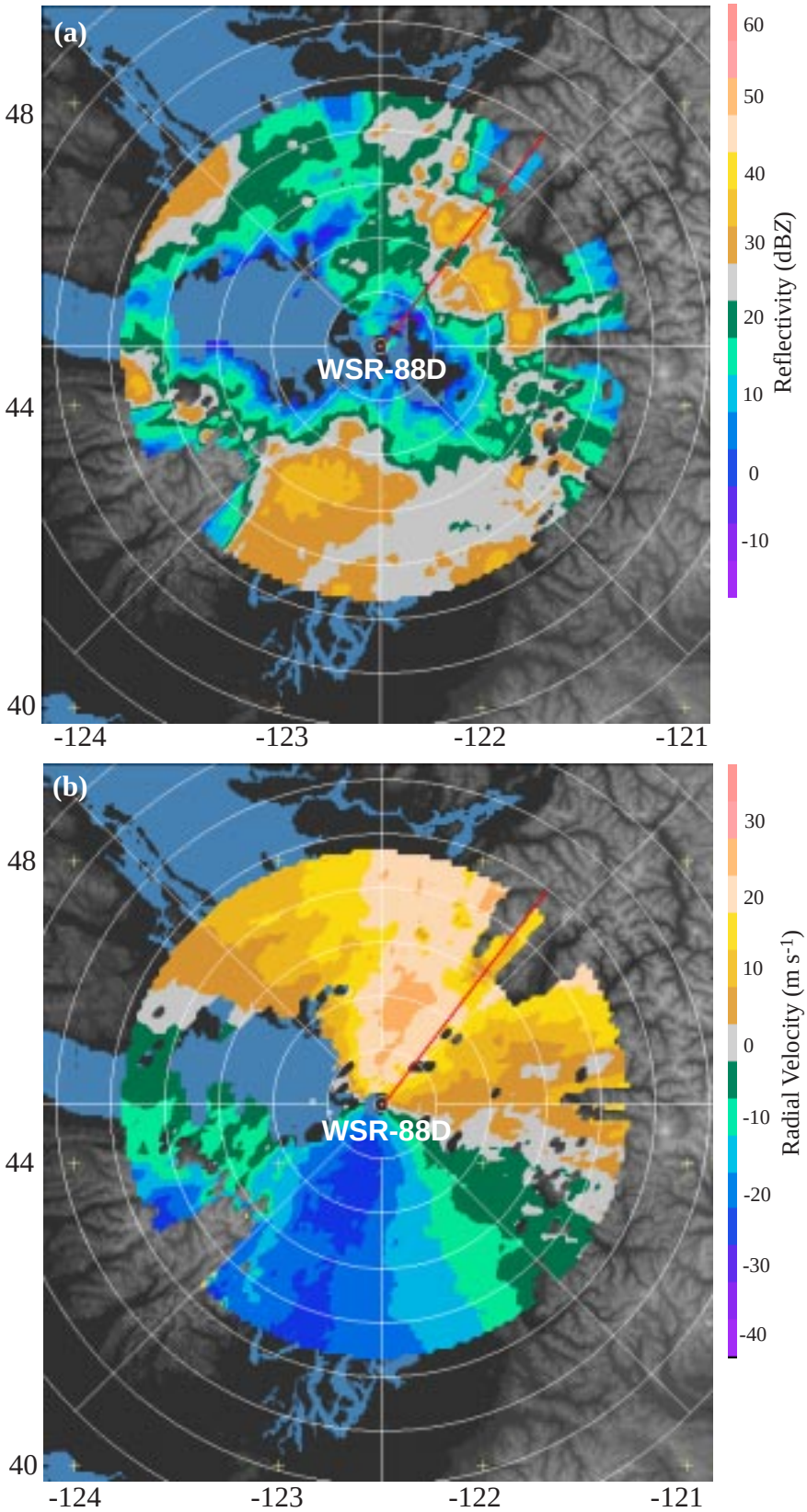

Figure 4. a) A horizontal cross-section of equivalent reflectivity (dBZ) taken at 0932 UTC January 23, 1998. The height of the plot is 1.5 km, with the background terrain height contoured in black and white. Range rings are spaced every 20 km and the cross marks indicate latitude and longitude intersects. b) Same as (a) except using radial velocity (m/s).

following examples of orographic, frontal, and convective precipitation over the Olympic Mountains and Cascade Range (Fig. 3) that have been displayed by *MountainZebra*.

Orographic Precipitation. At 0932 UTC January 23, 1998, several orographic precipitation mechanisms were influencing the intensity and distribution of precipitation over Western Washington. Horizontal cross-sections at 1.5 km altitude of radar reflectivity (Fig. 4a) and radial velocity (Fig. 4b) indicate winds from the south-southwest and a pattern of widespread precipitation that surrounds the radar site at Camano Island. The rain shadow of the Olympic mountains is evident in the weak echo region aligned downwind of the mountains from 80 km west to 40 km southeast of the radar. This is produced as strong subsidence to the lee of the Olympics adiabatically warms the air mass and suppresses precipitation.

Though the precipitation is suppressed in this region, it is enhanced as the flow impinges on the Cascade Range. A vertical cross-section of reflectivity taken from the radar to the northeast (indicated by the red line segment in Fig. 4a and 4b) reveals a region of enhanced precipitation over the windward slopes of the underlying terrain. This region is centered between 50 km and 65 km range along the radial (Fig. 5a). The same cross-section taken through the radial velocity field (Fig. 5b) shows that the flow is partially blocked by the terrain and radially convergent in this region and that the precipitation is orographically

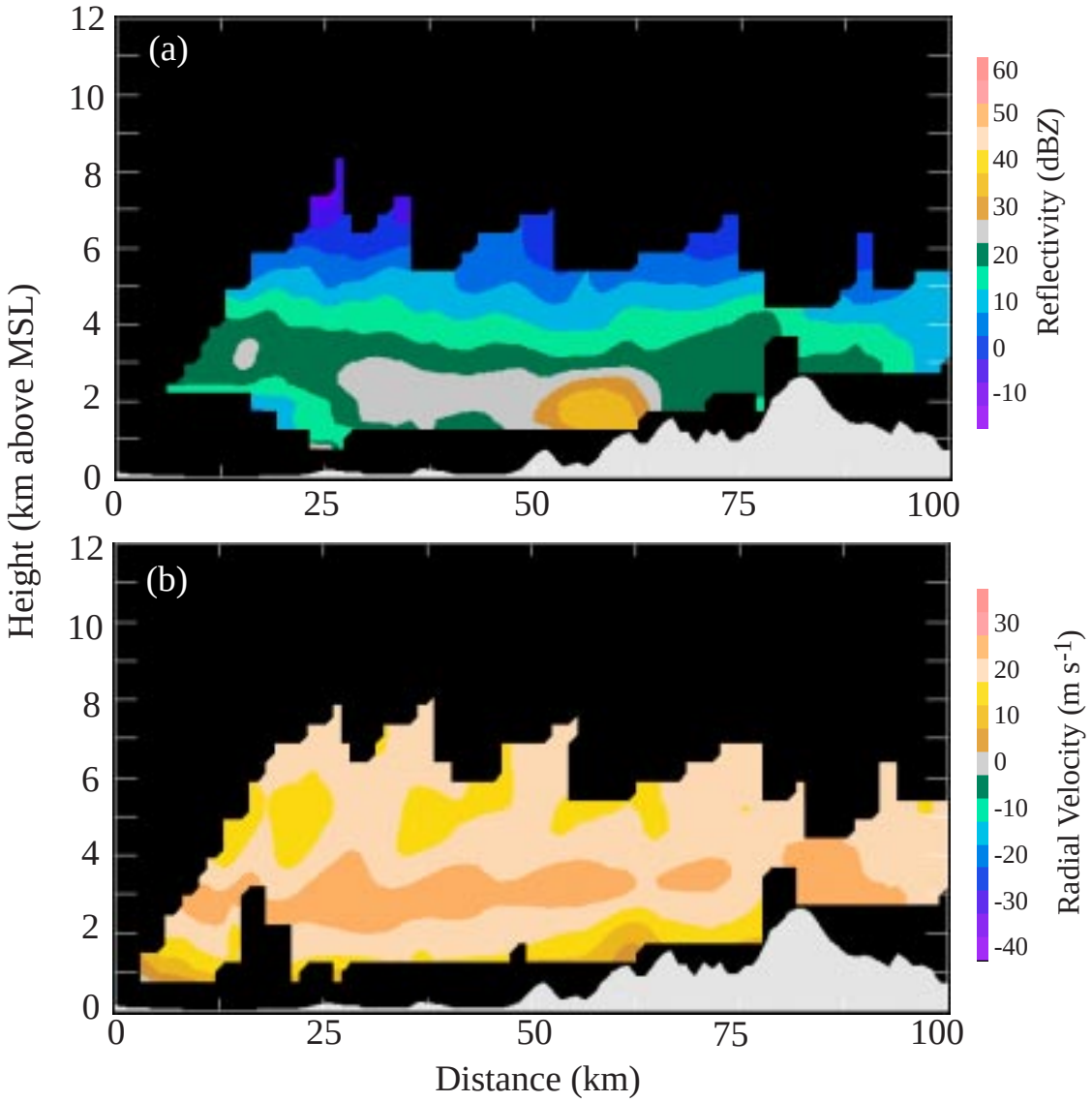

Figure 5. a) A vertical cross-section of dBZ taken at 0932 UTC January 23, 1998, from Camano Island to the northeast as indicated by the red segment in Fig. 4. The axis ranges from 0 to approximately 100 km in the horizontal and 0 to 12 km in the vertical. The underlying terrain profile is shown in light grey. b) Same as (a) except using radial velocity (m/s).

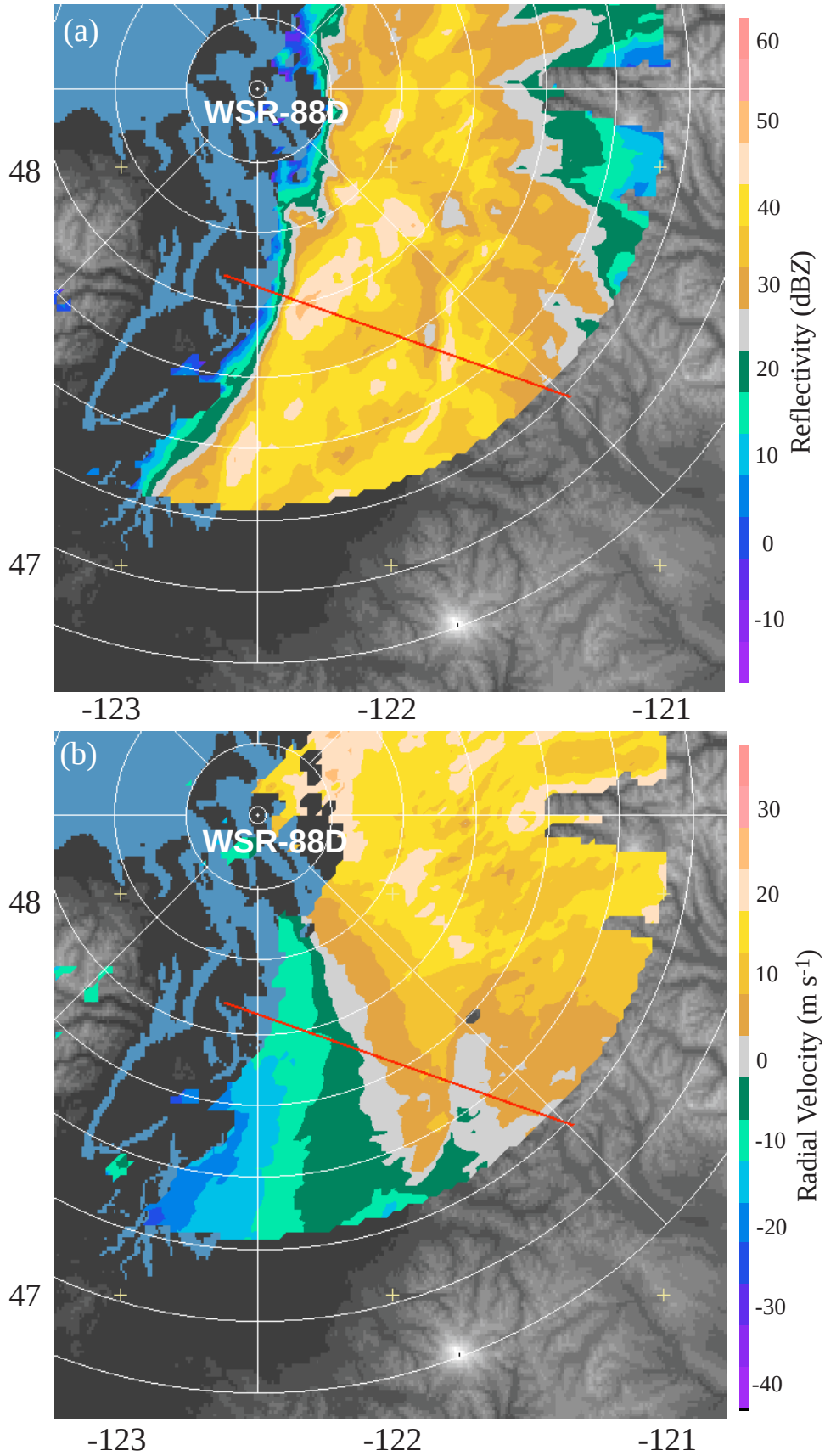

Figure 6. a) Horizontal cross-section of dBZ taken at 1315 UTC October 29, 1998, at an elevation of 2.0 km. b) Same as (a) except using radial velocity (m/s). Vertical cross section is indicated by the red segment.

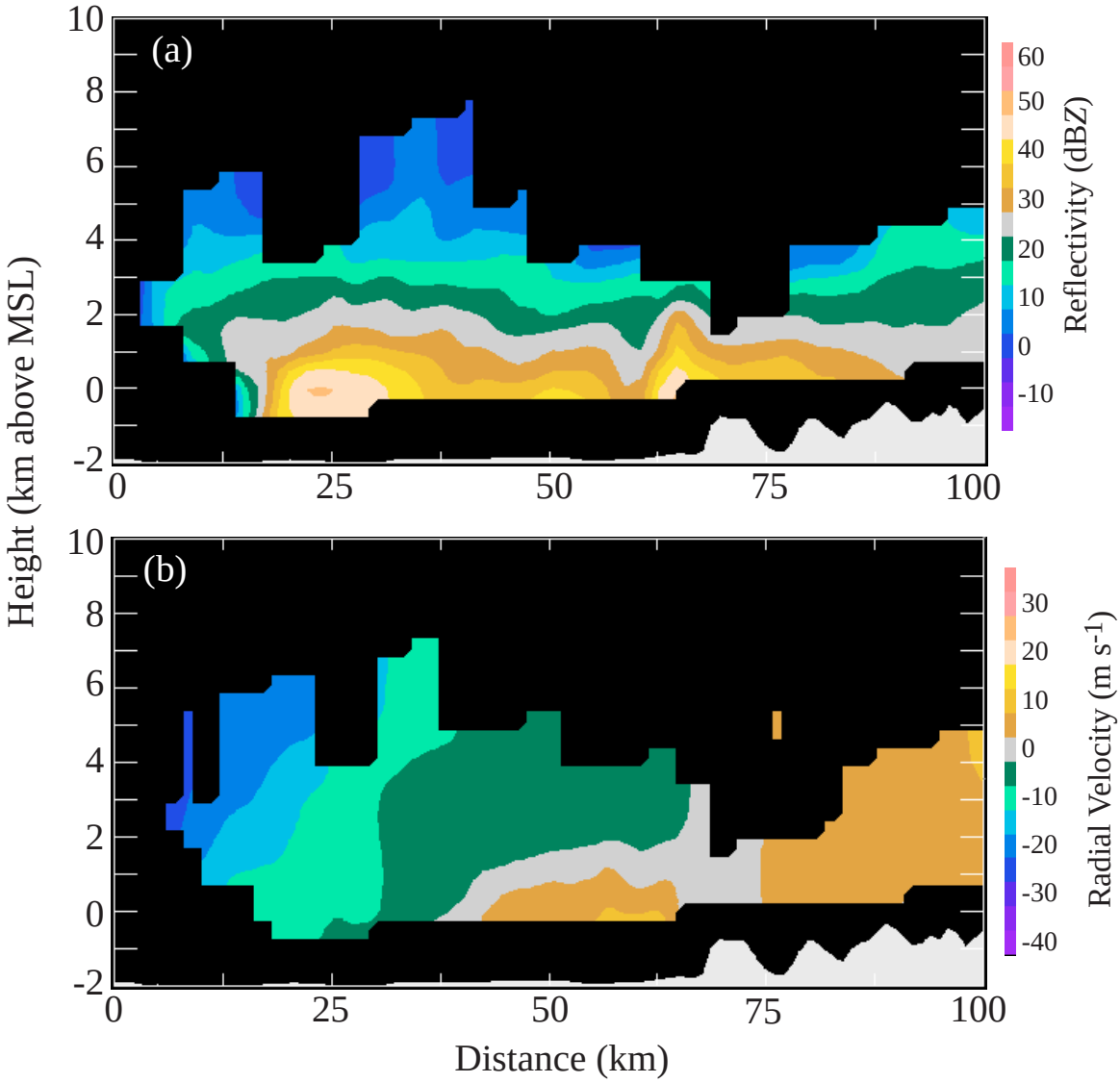

Figure 7. a) Vertical cross-section of dBZ taken perpendicular to the front through the most intense precipitation core as shown in Fig. 6. The underlying terrain is again superimposed. b) Same as in (a) except using radial velocity.

enhanced. Thus, overlaying radar fields with the topography in vertical cross-sections facilitates the interpretation and identification of orographic enhancement. Overlaying radar volumes with topography is also advantageous when assessing data quality. In this example, we note in both Fig. 5a and 5b that the lowest scan is blocked or partially blocked by Mt. Baker (the tallest peak in the terrain profile). We also note that blocks of data have been removed by the radar processor over these mountain slopes that are exposed to the radar.

Also if interest in this example is the evidence of lee gravity waves in the radial velocity field between 3 and 7 km height (Fig. 5b). At 3 km altitude, we note a layer of maximum radial velocity (> 25 m/s) that spans most of the cross-section. Above this layer, we observe spatial oscillations in the radial velocity field, both horizontally and vertically. A time-lapse loop of this cross-section indicates that the radial velocity perturbations remain quasi-stationary with time, indicating that this structure is driven by gravity waves.

Cold Frontal Precipitation. On 29 October 1997, a strong frontal system produced significant precipitation over Western Washington. At 1315 UTC, a cold front was oriented nearly north-south, approximately 50 km upstream from the Cascade Range. Fig. 6a contains a horizontal cross-section through the reflectivity field at an altitude of 2 km and Fig. 6b contains the radial velocity field. The horizontal reflectivity structure of the frontal zone closely resembles structures documented by Hobbs *et al.* (1980), characterized by long, narrow cold-frontal rainbands and embedded precipitation cores. Ahead of the front, however, the rainbands are less organized. The structure of these rainbands is better interpreted with some knowledge of the vertical structure

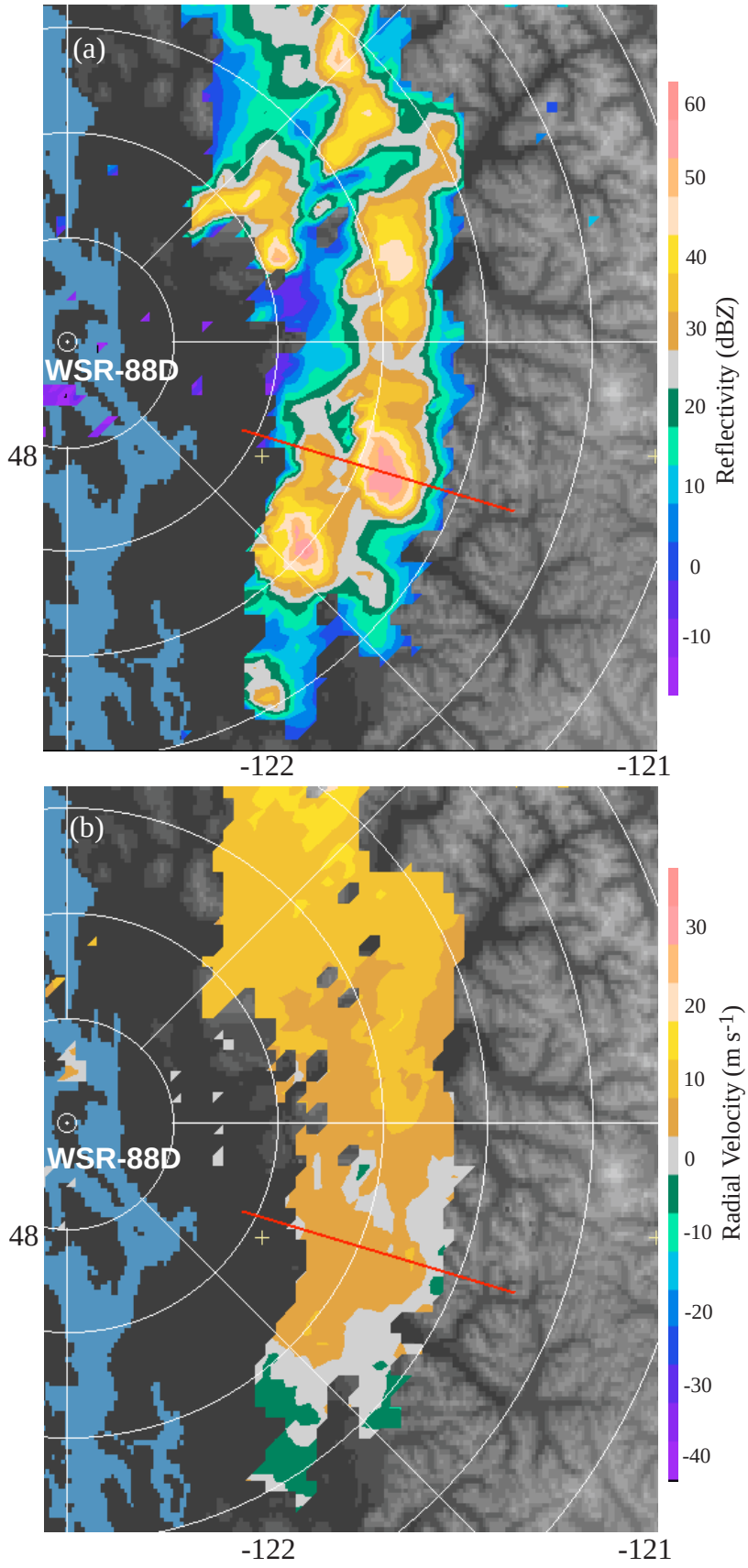

Figure 8. a) Horizontal slice through the equivalent reflectivity field at 3 km altitude on 6 August 1997, 23:59 UTC. Note the location of the vertical cross-section, as shown by the red segment. b) Radial velocity (m/s) slice at the same time and altitude.

of the precipitation and of the underlying topography. In order to examine the vertical structure of this system, we draw a cross-section west-northwest to east-southeast through the heaviest precipitation core and into the prefrontal rainbands. The vertical cross-section through the reflectivity field, shown in Fig. 7a, depicts upslope enhancement at x=63 km due to the steep slope of the terrain. In the frontal zone, we find a structure similar to that described by classical conceptual models of cold fronts (Browning, 1986), with an heavy precipitation core at the leading edge of a frontal boundary. The frontal boundary, as defined by the reflectivity echo, slopes upward between x=5 and x=25 km. The horizontal cross-section of radial velocity field (Fig. 6b) indicates a tongue of radially outbound flow extending southward from 140 azimuth and 80 km range along the windward side of the Cascade Range. By overlaying the radial velocity cross-section with the terrain profile (Fig 7b), we see that this effect is strongest along the base of the range (from 50 to 65 km along the cross-section), providing evidence that this circulation is mechanically forced by the orography.

Convective Precipitation. Fig. 8a is a constant

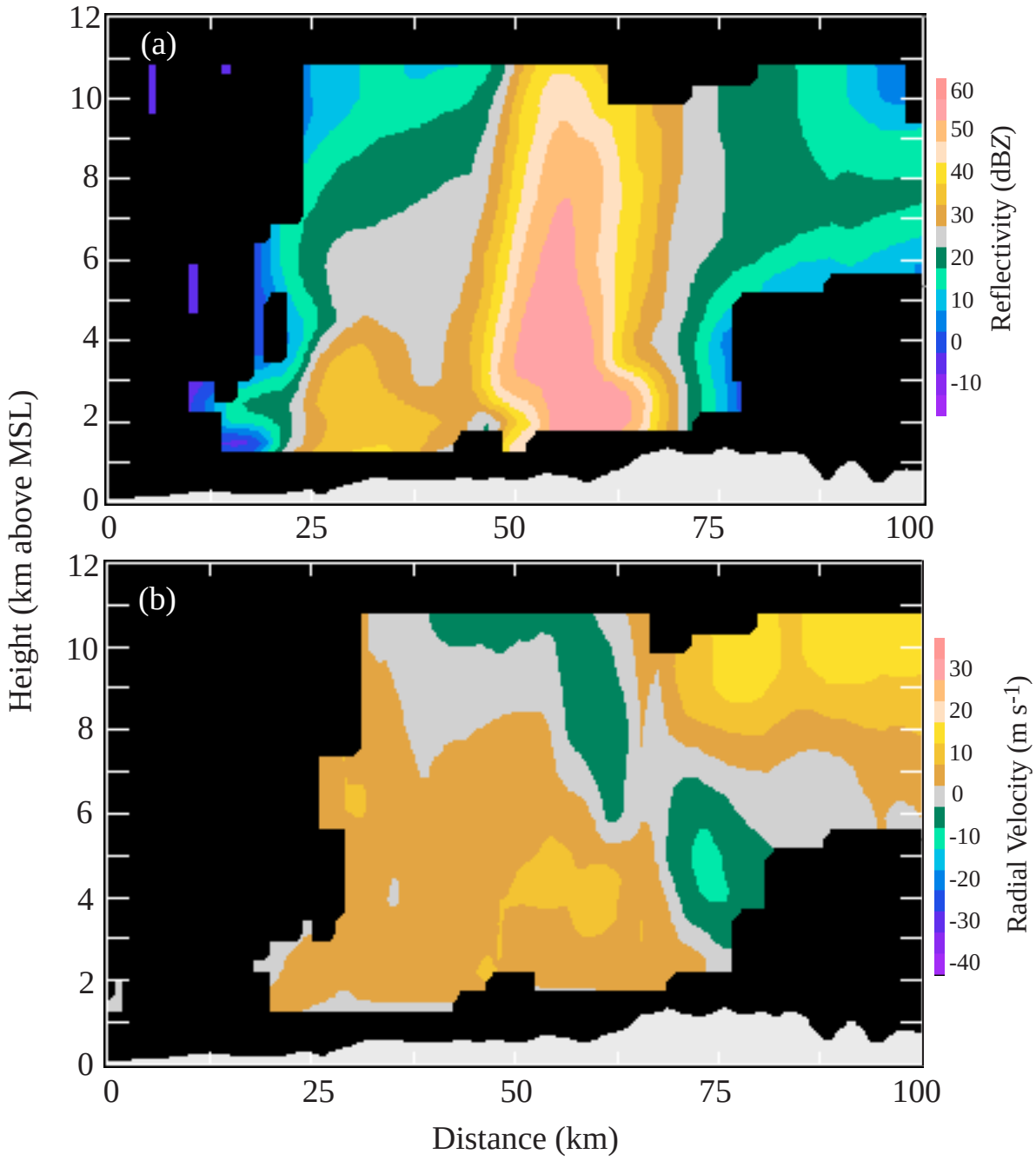

Figure 9. Vertical cross-sections of (a) equivalent reflectivity (dBZ) and (b) radial velocity (m/s) from west-northwest to east-southeast along the segment shown in Fig. 8.

altitude cross-section of reflectivity at 3 km altitude, through a line of thunderstorms that developed on the at 2359 UTC August 6,1997. Approximately two hours prior, the same thunderstorms moved east-northeast through the Seattle Metropolitan area, with reports of 0.47 in. of precipitation in approximately 30 minutes and marble-sized cone-shaped graupel. As the thunderstorms impinged on the windward slopes of the Cascade Range, they intensified. In Fig. 8b, we see that there is strong radial convergence at the leading edge of the line, especially at an azimuth of 115 and a range of 75 km. This strong convergence is collocated with the strongest convective cell in the reflectivity field. Vertical cross-sections of reflectivity and radial velocity taken from west-northwest to east-southeast through this cell indicate a well-defined multicellular storm structure. The echo tops reach approximately 12 km, with a 55 dBZ reflectivity core extending from the surface to 8 km. Behind the convective core, a stratiform region has begun to develop, with some indication of ice particles being detrained from the updraft region. The radial velocity field in Fig. 9b indicates strong storm-top divergence, with a significant updraft tilt and front-to-rear flow.

One peculiarity of this storm is the modification of its structure by the terrain. As seen in Fig. 9a, the base of the reflectivity core is not aligned vertically with the rest of the core. The orographic profile indicates that the base is collocated with a local valley or lowland, just upstream of a rather steep slope. We speculate that the topography blocked the low-level flow, altering the updraft and downdraft circulations, gust front and cold pool dynamics of this storm.

4. CONCLUSIONS

The examples shown here demonstrate the value added to the interpretation of a variety of precipitation processes in the context of orographic forcing by *MountainZebra*, an augmentation of NCAR's *Zebra* software that superimposes radar data on the terrain profile. *MountainZebra* can display gridded observational data sets or derived fields in both real-time and post-analysis applications. Real-time WSR-88D level II data accessed via NSSL's RIDDS system can be used as input to a chain of programs that reformats and interpolates radar data for display in *MountainZebra*. By interpolating radar volumes to a Cartesian grid and overlaying cross-sections with terrain profiles, optimal visualization of orographically-induced precipitation system structures can be achieved. This visualization technique can be expanded to include mesoscale model fields, satellite imagery, and other geophysical fields for research and operational applications in mountain meteorology.

ACKNOWLEDGEMENTS

The authors appreciate the collaboration of Brad Colman and Chris Hill of the Seattle National Weather Service Forecast Office. This research was supported in part by the National Science Foundation Grant #ATM-9409988 and by JISAO Cooperative Agreement #NA67RJ0155. This is JISAO contribution number 576. The high-resolution USGS elevation data were provided by NCAR's Scientific Computing Division.

REFERENCES

Barnes, S. L., 1980: Report on a meeting to establish a common Doppler radar data exchange format. *Bull. Amer. Meteor. Soc.*, **61**, 1401-1404.

Browning, K. A., 1986: Conceptual models of precipitating systems. *Wea. Forecasting*, **1,** 23-41.

Corbet, J., C. Mueller, C. Burghart, K. Gould, and G. Granger, 1994: Zeb: software for integration, display, and management of diverse environmental datasets. *Bull. Amer. Meteor. Soc.*, **75**, 783-792.

Crum, T. D., and R. L. Alberty, 1993: Recording, archiving, and using WSR-88D data. *Bull. Amer. Meteor. Soc.*, **74**, 645-653.

Hobbs, P. V., T. J. Matejka, P. H. Herzegh, J. D. Locatelli, and R. A. Houze, Jr., 1980: The mesoscale and microscale structure and organization of clouds and precipitation in midlatitude cyclones. I: A case study of a cold front. *J. Atmos. Sci.*, **37,** 568-596.